Nature Meets Infrastructure

The Role of Mangroves in Strengthening Bangladesh's Coastal Flood Defenses

Gijón Mancheño, Alejandra; Jafino, Bramka A.; Hofland, Bas; van Wesenbeeck, Bregje K.; Kazi, Swarna ; Urrutia , Ignacio

DOI
10.3390/su17041567

Publication date
2025

Document Version
Final published version

Published in
Sustainability

Citation (APA)
Gijón Mancheño, A., Jafino, B. A., Hofland, B., van Wesenbeeck, B. K., Kazi, S., & Urrutia , I. (2025). Nature Meets Infrastructure: The Role of Mangroves in Strengthening Bangladesh's Coastal Flood Defenses. *Sustainability*, *17*(4), Article 1567. https://doi.org/10.3390/su17041567

sustainability

MDPI

Article

Nature Meets Infrastructure: The Role of Mangroves in Strengthening Bangladesh's Coastal Flood Defenses

Alejandra Gijón Mancheño [1,2,*], Bramka A. Jafino [2], Bas Hofland [1], Bregje K. van Wesenbeeck [1,3], Swarna Kazi [2] and Ignacio Urrutia [2]

[1] Department of Hydraulic Engineering, Faculty of Civil Engineering and Geosciences, Delft University of Technology, Stevinweg 1, 2628 CN Delft, The Netherlands
[2] World Bank, 1818 H Street, Washington, DC 20433, USA
[3] Department of Ecosystems and Sediment Dynamics, Deltares, P.O. Box 177, 2600 MH Delft, The Netherlands
* Correspondence: a.gijonmancheno-1@tudelft.nl

Abstract: Mangroves have been used for coastal protection in Bangladesh since the 1960s, but their integration with embankment designs has not been fully explored. This paper investigates the effect of existing mangroves on required embankment performance, with a focus on the wave-damping effect of mangroves. Existing mangroves reduce the required thickness of embankment revetment by up to 16–30% in the west, 47–82% in the central region, and 53–77% in the east. Notable mangrove sites include the belt south of polder 45 (Amtali), with an average width of 1.77 km, and the Kukri-Mukri polder, with an average width of 1.82 km. These mangroves reduce the need for thick slope protection, allowing the replacement of concrete revetments with softer materials, such as clay or grass, combined with mangrove foreshore. Additional large mangrove belts are found in Sandwip and Mirersarai. By replacing or reducing revetment requirements, mangrove forests can minimize carbon emissions from construction while providing carbon sequestration and other ecosystem services. This study can inform future sustainable investments in coastal protection systems by identifying areas where mangroves offer the greatest wave-damping benefits, which could be focus of follow-up feasibility studies.

Keywords: mangroves; nature-based solutions; hybrid engineering; coastal embankments; coastal protection; sustainable investments

Academic Editor: Faccini Francesco

Received: 19 January 2025
Revised: 7 February 2025
Accepted: 11 February 2025
Published: 13 February 2025

Citation: Gijón Mancheño, A.; Jafino, B.A.; Hofland, B.; van Wesenbeeck, B.W.; Kazi, S.; Urrutia, I. Nature Meets Infrastructure: The Role of Mangroves in Strengthening Bangladesh's Coastal Flood Defenses. *Sustainability* **2025**, *17*, 1567. https://doi.org/10.3390/su17041567

1. Introduction

Bangladesh faces significant risk from extreme weather events given its frequent flood exposure and large population living in low-lying areas [1]. To address increasing flood risks linked to climate change [2], flood safety standards of the country's coastal embankment system are being upgraded through the Coastal Embankment Improvement Project Phase 1 (CEIP-1). Part of these improvements includes evaluating the use of mangroves on the seaward side of embankments to reduce the impact of extreme events. Mangroves—tropical trees and shrubs adapted to low-energy intertidal coastal and estuarine environments—naturally mitigate flood damages by reducing the impact of waves and surges [3–5]. Mangroves are naturally present along Bangladesh' coastlines and have also been planted as a flood defense measure since the 1960s [6]. However, existing forests have not yet been fully integrated into embankment designs, suggesting significant opportunities to optimize embankment reinforcements. Existing coastal embankments consist of an earthen core shielded by concrete revetment blocks to protect the core against wave impacts (as shown in Figure 1 of Crawford et al. [7]). Raising embankment heights to meet higher

safety standards entails significant costs. However, the protective effect of mangroves presents an opportunity to reduce embankment heights and revetment requirements [8], while also delivering co-benefits such as carbon sequestration and ecosystem services [9,10].

While several local studies have highlighted the benefits of mangrove belts for reducing coastal flood risk in Bangladesh [8,11], no comprehensive, nationwide assessment exists on their potential for wave reduction and the resulting implications for coastal protection infrastructure design. Past research studies have shown that a 500-m-wide mangrove belt can reduce current speeds by up to 90% [11] and attenuate waves by 30–55% for the embankment design conditions of Bangladesh, depending on wave and forest characteristics [8]. This wave attenuation alleviates stress on coastal structures. For example, forests of *Sonneratia apetala* with widths up to 1 km could reduce wave heights by 7–55%, potentially allowing for reductions in embankment block sizes of 13–46% [8]. Despite these findings, existing studies are primarily localized and focused on specific regions or events, leaving a gap in our understanding of how these protective effects could be optimized and applied across the entire coastline of Bangladesh. A nationwide study on mangrove belt effectiveness for wave attenuation and implications for engineering designs could thus provide critical insights, promote coastal resilience, and improve infrastructure design in the face of intensifying climate threats.

This paper provides estimates of how mangrove belts could influence coastal embankment designs in Bangladesh. This is illustrated by digitizing current mangrove belts along embankments and assessing how these belts reduce wave impacts using an adapted form of the model of Mendez and Losada [12]. Then, wave reduction data are applied to adjust embankment specifications, such as crest height, slope revetment thickness, and erosion at the toe, following the approach of Gijón Mancheño et al. [8]. The study pinpoints areas where extensive mangrove belts already exist and can be incorporated into potential embankment reinforcement designs. These findings provide direction for future investments and identify research needs to fully integrate mangroves into coastal protection strategies.

2. Materials and Methods

2.1. Description of Mangrove Context in Bangladesh

The southwestern coast of Bangladesh is home to 60% of the Sundarbans, the world's largest continuous mangrove forest. The Sundarbans forest hosts approximately 27 species of mangroves [13], with *Heritiera fomes* (Sundri), *Excoecaria agallocha* (Gewa), and *Ceriops decandra* (Goran) constituting 95% of the forest's vegetation [13,14]. Despite its designation as a protected natural reserve [14], the Sundarbans have experienced a yearly shrinkage of 0.08% from 1996 to 2016 [15], primarily due to over-exploitation, deforestation, pollution, and natural disasters [16,17].

Ancient maps indicate that the Sundarbans used to extend further towards the mouth of the Meghna river, but the forest has been extensively deforested since the 19th century [18,19]. To counteract coastal flooding along deforested areas, mangrove plantations have been established since 1966 [6]. Over recent decades, these plantations have reached biomass levels comparable to natural forests, though they lack similar species diversity [15]. Initially, monoculture planting focused on pioneer species, particularly *Sonneratia apetala* (Keora) and *Avicennia officinalis* (Baen) [6]. In recent years, additional species, such as *Heritiera fomes*, have been introduced into several older plantations to enhance biodiversity [20]. Nevertheless, planted areas have declined in size at an average rate of 0.47% annually from 1996 to 2016 [15]. Mangrove losses underscore the difficulty of preserving and expanding mangrove habitats amid environmental and anthropogenic pressures.

On the southeast coast, fragmented and degraded fringe mangroves are dominated by *Sonneratia apetala*, *Avicennia officinalis*, and *Excoecaria agallocha* [20]. The once-thriving Chakaria

Sundarbans forest has suffered extensive degradation since the 1970s due to shrimp farming, over-harvesting, and hydrological changes [21]. Restoration initiatives, including the planting of 600,000 saplings in 2019, aimed to restore mangrove cover in this region [22]. Additionally, afforestation efforts started in the 1970s in the Mirersarai area and have shown promising results. For example, *Sonneratia apetala* demonstrated extensive growth and regeneration [22]. Surveys of plantations that were established with only two species (*Sonneratia apetala* and *Avicennia officinalis*) in the beginning, later showed the presence of up to eight mangrove species, suggesting natural colonization in these areas [23].

2.2. Identification of Mangrove Locations

We have selected mangrove belts along the different coastal zones in the country according to the following criteria: mangrove belts should be (1) located on the waterside of embankments, (2) display mangrove presence on the foreshore, and (3) should not overlap with active agriculture, aquaculture, and residential areas. Polygons enclosing mangrove sites are digitized in Google Earth and the mean width and length of the polygons are calculated in ArcMap, version 10.8.2 based on the geometry of a rectangle with equivalent surface area. The potential benefits of the different identified areas are estimated considering their width and the hydrodynamic design conditions of nearby embankments [24] to estimate their wave-reduction potential. For the wave attenuation assessment, we assumed that waves were perpendicular to the longest side of the rectangles.

2.3. Model of the Effect of Mangroves on Embankment Designs

Since we are considering afforesting sites that extend up to several kilometers (<2 km of average width), mangroves would cause only a very limited reduction in surge levels (between 0–0.2 m per km). We therefore focus on the effect of mangroves on short wave reduction and on the design requirements of coastal embankments. For this, we apply the approach of Gijón Mancheño et al. [8] to estimate wave attenuation by mangrove fringes, and calculate how these fringes could reduce the embankment crest height, the size of the slope protection (revetment) blocks, and the bed erodibility of the toe of the structure. The main equations of the approach are presented below. For the model validation, see Gijón Mancheño et al. [8].

Wave propagation is calculated using the wave energy balance [12]:

$$\frac{\partial E c_g \cos\theta}{\partial x} = -\epsilon_b - \epsilon_v \tag{1}$$

where E is the wave energy per unit area (J/m^2), c_g is the group celerity (m/s), θ is the mean wave direction (rad), ϵ_b represents wave dissipation due to depth-induced breaking (W/m^2), and ϵ_v represents wave dissipation by mangrove trees (W/m^2). Wave dissipation by bed friction is neglected under the assumption that it is much smaller than energy dissipation by breaking or the presence of aquatic vegetation [12]. Equation (1) is implemented with a forward stepping scheme from the seaside boundary towards the forest with a grid size Δx and a fixed water level, based on Mendez and Losada [12].

Wave attenuation due to depth-induced breaking is estimated with the approach of Thornton and Guza [25]:

$$\epsilon_b = \frac{3\sqrt{\pi}}{16}\rho_w g \frac{B^3 f_p}{\gamma_{br}^4 h^5} H_{rms}^7 \tag{2}$$

where f_p is the peak frequency (s^{-1}), ρ_w is the water density (kg/m^3), g is the acceleration of gravity (m/s^2), H_{rms} is the root mean square wave height (m), and B (-) and γ_{br} (-) are empirical coefficients that are set to the default values used by Mendez and Losada [12]: $B = 1$ and $\gamma_{br} = 0.6$.

Wave energy loss due to the presence of a mangrove forest is computed as the work of the drag forces acting on the trees:

$$\epsilon_v = \frac{1}{T_p}\overline{\int_{-h}^{-h+h_v} \frac{1}{2}\rho_w c_{D,w} b_v(z) N_v u_w(z)^3 dz dt} \quad (3)$$

where T_p is the peak wave period (s), t is the time (s), b_v is the integrated tree width at an elevation z from the ground (m), which corresponds with the sum of the widths of all branches or roots at a given height z, and N_v is the tree density per unit area (trees/m^2). Equation (3) is integrated numerically over the vertical coordinate z (m) over cells with a height Δz and varying width $b_v(z)$ and wave orbital velocity $u_w(z)$. $c_{D,w}$ is the bulk drag coefficient, $u_w(z)$ is the orbital velocity associated to the root-mean-square wave height (m/s), h is the water depth (m), and h_v is the tree height (m). Large-scale experiments with willow trees provided values of $c_{D,w} = 0.7 - 2$ [26].

The embankment height is selected to ensure that the overtopping discharge remains below a critical threshold, q_{max} (m^3/m/s) using the formula of EurOtop [27]:

$$q = \sqrt{gH_{m0}^3}\frac{0.026}{tan(\alpha)}\gamma_b \epsilon_{m-1.0} e^{-\left(2.5\frac{h_{crest}-h}{\epsilon_{m-1.0}H_{m0}\gamma_b\gamma_f\gamma_\beta\gamma_v}\right)^{1.3}} \quad (4)$$

where q is the overtopping discharge per meter (m^3/m/s), α is the angle of the outer slope (-), $\epsilon_{m-1.0}$ is the breaker parameter (-), γ_b is the influence factor for a berm (-) , γ_f is the influence factor for roughness elements on the slope (-), γ_β is the influence factor for oblique wave attack (-), γ_v is the influence factor for vertical wall (-), h_{crest} is the crest level (m), and h is the water depth at the embankment toe (m).

The thickness of the slope protection is estimated with the formulation of Pilarczyk [28,29].

$$\frac{H_{m0}}{\Delta D} = \frac{F\cos\alpha}{\epsilon_{m-1.0}^b} \quad (5)$$

where H_{m0} is the spectral significant wave height at the toe of the structure (m), D is the thickness of the cover layer (m), Δ is the relative density of concrete with respect to water (-), F is a stability factor between 3-6 for a revetment formed by concrete blocks (-), and b is an exponent equal to 0.67 for semi-permeable block revetments (-).

The shear stresses ($\tau_{b,w}$) acting on the embankment toe are estimated with Equation 6, as a proxy for sediment erosion:

$$\tau_{b,w} = \frac{1}{4}\rho_w f_w u_{w,b}|u_{w,b}| \quad (6)$$

where $u_{w,b}$ is the orbital velocity (m/s) associated to the root mean square wave height at the sea bottom ($z = -h$), f_w is the wave friction factor (-) [30]:

$$f_w = min\left(\exp\left(-6 + 5.2\left(\frac{u_{w,b}}{2.5 d_{n50}\omega_m}\right)^{-0.19}\right), 0.3\right) \quad (7)$$

with d_{n50} being the mean grain size (m) and ω_m the mean wave frequency (rad/s).

2.4. Modelling Parameters

The study of Gijón Mancheño et al. [8] evaluated the effect of mangroves for selected polders at the center of Bangladesh, whereas this study considers the variation in hydrodynamic conditions across all coastal zones. For each region (west, center, east—see Figure 1), the hydrodynamic design conditions are obtained from IWM [24] for a return period of

25 years. Water levels include +1 m of sea level rise by 2050, corresponding with the worst-case scenario due to climate change [8]. The hydrodynamic conditions used in the simulation are summarized in Table 1. Wave heights and surges are smallest on the west and central regions, and largest at the east coast of Bangladesh.

Table 1. Hydrodynamic design conditions of embankments at the locations of Figure 1. For each region, the maximum and minimum value of the design water levels (25-year return period, including +1 m due to sea level rise by 2050) and wave height (25-year return period) are calculated from the data of IWM [24].

Location	Surge_{min} [m]	Surge_{max} [m]	H_{min} [m]	H_{max} [m]
West	3.8	4.2	1.0	1.0
Center	3.6	4.4	0.9	3.2
East	4.5	5.2	2.2	3.9

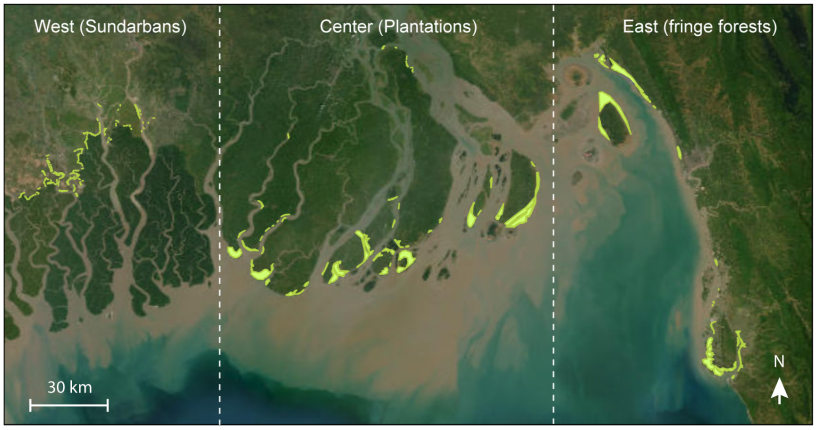

Figure 1. Location of existing mangroves on the waterside of embankments (light green polygons) in Bangladesh at the west, center, and east regions. Basemap by Google Earth (2024).

The IWM report [24] does not specify the wave period corresponding to the given wave height but assumes a wave steepness of $s_0 = 0.05$, where wave steepness s_0 is defined as the ratio of wave height H_{m0} to wavelength L. For our wave attenuation calculations, we adopt this same steepness to evaluate the impact of mangroves under design conditions for the structures. The wavelength is calculated as $L = H_{m0}/s_0$, and the wave period is then determined using the dispersion relation from linear wave theory, factoring in the design water level.

The vegetation properties (Table 2) are obtained combining the model for the vegetation surface area of Gijón Mancheño et al. [8] with mangrove geometrical properties measured in Bangladeshi plantations by Uddin et al. [23], at Domkhali, Moghadia, and Bamonsundar (north of Chittagong), summarized in Table 2. Vegetation characteristics likely differ at other sites, specially at the west, but we lacked data to include such spatial variations.

Table 2. Vegetation properties from plantations with ages between 20–29 years old at Domkhali, Moghadia, and Bamonsundar from Uddin et al. [23].

Variable [Units]	Minimum Value	Maximum Value
Density [trees/m^2]	0.07	0.15
DBH [m]	0.23	0.25
h_v [m]	10.5	11.8

Within the model, we assume a constant water depth through the vegetation, equal to the surge levels from IWM [24]. We consider mangrove belt widths varying between 10–2000 m. Attenuated wave heights are used to calculate the embankment properties. The crest height is calculated using Equation (4) to reach an overtopping rate of 5 l/m/s with embankment slopes of 1:8, armor layers (corresponding with $\gamma_f = 0.55$), and a berm (with $\gamma_b = 0.89$), perpendicular wave incidence (so $\gamma_\beta = 1$), and no vertical walls ($\gamma_v = 1$). The size of the slope protection is calculated using Equation (5), with a permeability of P = 0.1, relative density of concrete blocks of $\Delta = 1.7$, an acceptable level of damage of $S = 2$, and a number of waves of $N = 500$. The shear stresses at the toe of an embankment are calculated assuming a grain size of $D_{n50} = 7$ µm in Equations (6) and (7).

3. Results

3.1. Identified Mangrove Belts

Locations of existing mangrove belts fronting embankments, are shown in Figure 1. The range of mangrove patch lengths (along the embankment), widths (in the direction across the embankment), and total surface area are shown in Table 3. Mangrove belts correspond with continuous areas showing mangrove presence between embankments and water bodies, excluding areas of aquaculture, agriculture and buildings (see Materials and Methods Section 2). Most identified mangrove sites are relatively narrow. In particular, out of the 255 identified sites, 159 had widths below 100 m, 99 had widths longer between 100 and 500 m, and only 32 had widths exceeding 500 m (see distribution in Figure 2). In total, the cumulative length of mangrove belts is 8 km, 27 km, and 16 km at the west, center, and east regions, respectively.

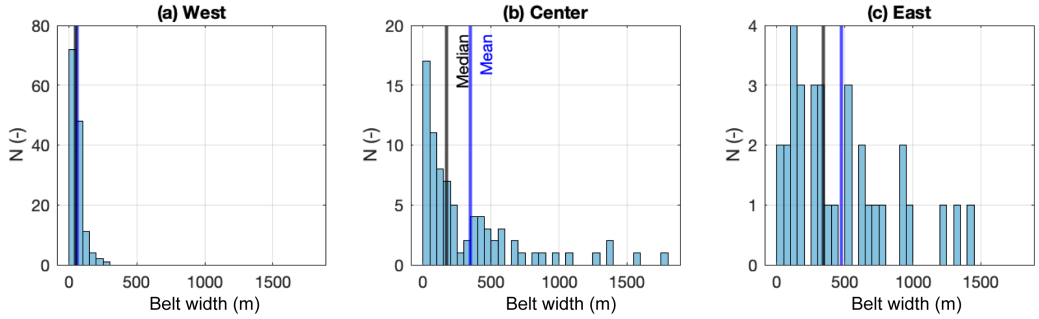

Figure 2. Histograms of mangrove forest belt width for the (**a**) west, (**b**) center and (**c**) east regions. The x-axis represents forest (cross-shore) width in meters, grouped in increments of 50 m, while the y-axis indicates the number of observations in each bin. Blue vertical lines mark the mean forest length, and black vertical lines indicate the median forest width for each region. The histograms highlight the distribution and central tendencies of forest width across the three regions.

Table 3. Characteristics of existing and potential sites where mangroves could be integrated into embankment designs, based on the areas shown in Figure 1. The table provides the maximum and minimum values of the average width and length of mangrove sites and their maximum and minimum areas.

Location	Width_{min} [m]	Width_{max} [m]	Length_{min} [m]	Length_{max} [m]	Area_{min} [m^2]	Area_{max} [m^2]
West	15	268	209	3898	3596	911,773
Center	11	1821	164	20,840	1842	26,419,582
East	13	1438	124	28,068	17,325	14,136,721

3.2. Effect of Mangrove Belts on Waves

Mangrove belts have large potential to reduce wind waves, especially at the center and east of the country (Figure 3). At the west, forest widths vary between 15–268 m, with most widths remaining below 100 m. For the average belt width of 60 m, wave transmission rates—defined as the ratio of wave height after it passes through a forest to the initial wave height at the forest's edge—vary between 92–96% (Figure 3a). The effect of such narrow mangrove belts is much smaller than the benefits provided by the neighboring Sundarbans, which are already accounted for in the input hydrodynamic conditions of the region (Table 1).

Mangroves have a larger potential to reduce wave heights at the center of Bangladesh (Table 3) relative to the west due to higher wave exposure (see the larger wave heights in Table 1) and longer mangrove widths (as indicated by the wider shaded gray areas/rectangles in Figure 3). For the average mangrove belt widths of 349 m, wave transmission ranges between 47–80%. For a maximum forest width of 1.82 km, wave transmission varies between 18–52%.

The east region shows similar results to the center of the country (Figure 3c). Overall, mangrove belts have an average width of 477 m, which is associated with a wave transmission of 43–69%. The longest belts reach widths of 1.4 km, for which wave transmission varies between 22–46%.

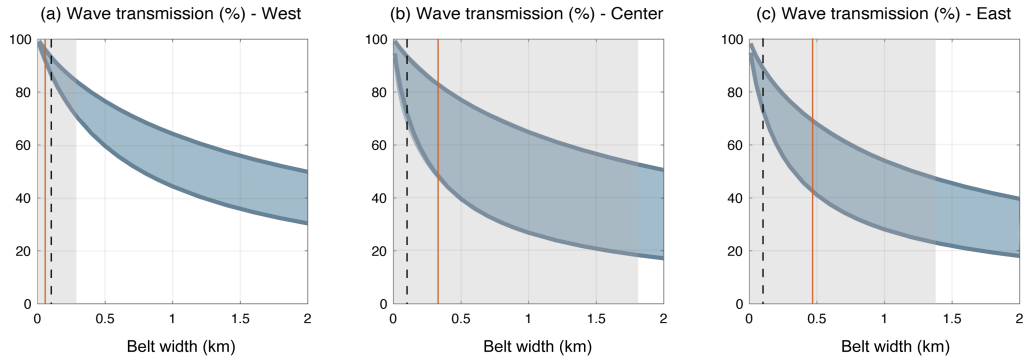

Figure 3. Wave transmission through mangrove belts (%) at (**a**) west, (**b**) center, and (**c**) east of Bangladesh. Blue areas show the range of wave reduction estimates for each belt width, based on the minimum and maximum values of Table 1. Gray areas show the available belt widths in the region, the black dashed line marks a belt width of 100 m, and the orange line indicates the average belt width.

3.3. Effect of Mangroves on Embankment Designs

At the west, mangrove belts have limited potential to reduce the wave-related components of the design, i.e., the revetment thickness (Figure 4b) and the shear stresses at the toe of the structure (Figure 4c), since identified mangrove sites are relatively narrow. With the average mangrove belt width of 60 m, the thickness of the revetment would decrease by 3–6%, and the shear stresses by 7–16%. For the maximum forest width of 268 m, the reduction in the revetment block thickness reaches up to 16–30%, and the reduction in the shear stresses up to 30–50%. Water level (and crest height) reduction remains below 4% (<0.13 m) for all modeled widths (Figure 4a) because the design water level is dominated by the surge, which is unaffected by mangroves in our model. However, even assuming the largest surge reduction rate ever observed in the field, of 0.2 m/km [31,32], the maximum surge reduction by these mangrove belts would be 0.06 m for the widest transect (268 m), which is less than 2% of the total water level.

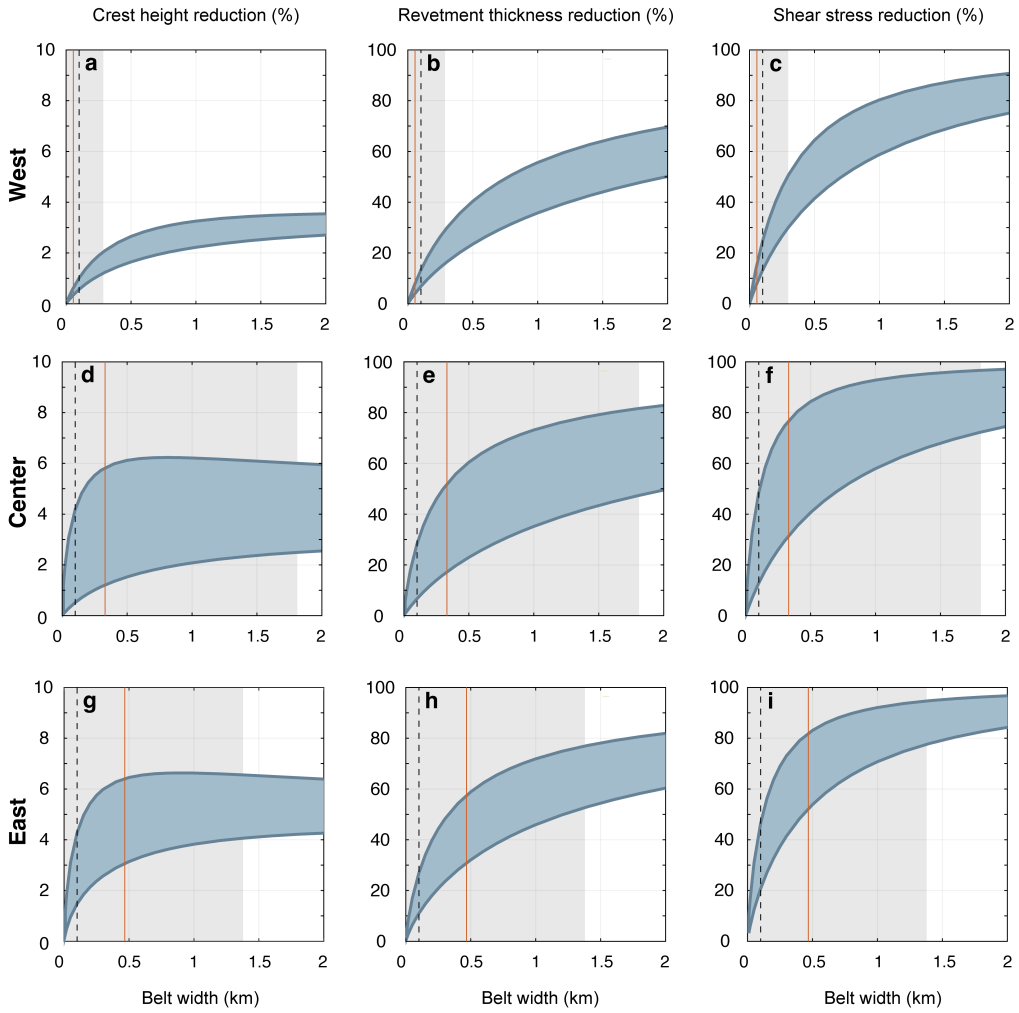

Figure 4. Effect of mangrove afforestation in the west, center, and east of Bangladesh, in terms of (**a**,**d**,**g**) crest height reduction, (**b**,**e**,**h**) reduction in the revetment thickness, (**c**,**f**,**i**) and reduction in the shear stresses. Blue areas show the range of wave reduction estimates for each belt width, based on the minimum and maximum values of Table 1. Gray areas show the available belt widths in the region, the black dashed line marks a belt width of 100 m and the orange line indicates the average belt width.

At the central region, mangroves can provide larger benefits by reducing the revetment (Figure 4e) and bank protection (Figure 4f). The average mangrove belt width of 349 m is associated with revetment thickness reductions of 17–52% and shear stress reductions of 30–78%. For the widest belt (1.82 km), the revetment reduction ranges between 47–82% and the shear stress reduction ranges between 71–96%. The effect of mangroves on design water levels and crest heights is still low for all forest widths, and crest height reductions due to the presence of a forest remain below 6%.

The east region shows similar results to the center of the country (Figure 4g–i). Overall, the average mangrove belt width of 477 m is associated to a revetment thickness reduction of 30–60%, and to a shear stress reduction of 53–83% at the toe of the structure. For the longest belt width of 1.4 km, the vegetation largely reduces the required revetment (53–77%) and shear stresses (79–97%). The east coast is exposed to the largest surge levels and wave heights (Table 1), and due to this exposure, mangroves tend to grow behind natural obstacles to wave action (such as the island of Sandwip). Water level reduction remains below 7% for all forest widths.

3.4. Polders with Most Potential for Mangrove Integration

The comparison between the effect of mangroves in the three regions can be seen in Figure 5, which shows the areas of most revetment reduction benefits in the center and east of Bangladesh.

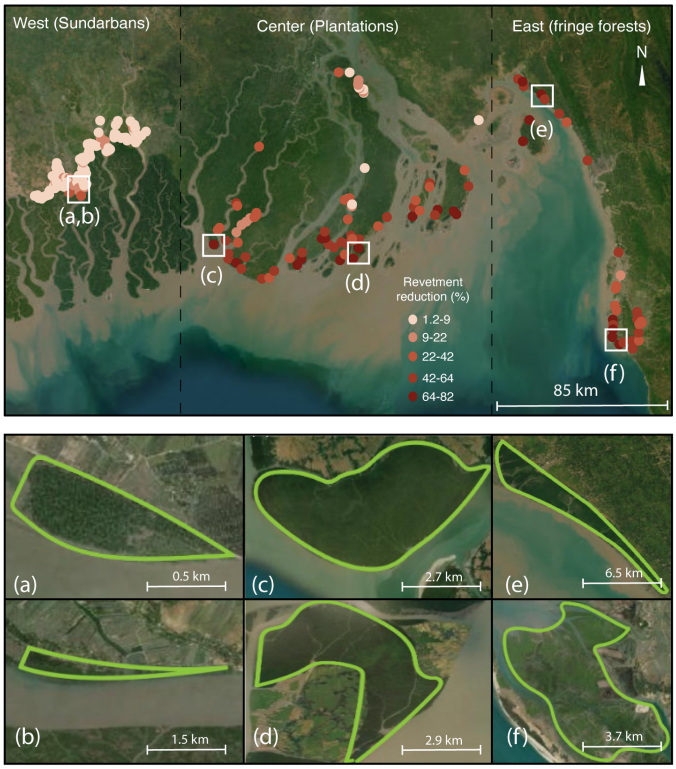

Figure 5. Potential revetment reduction in Bangladesh (%), corresponding with the upper values of wide mangrove belts that could reduce embankment design requirements in Bangladesh in Figure 4, with close-ups of the mangrove belts of (**a**) Shamnagar (polder 7/1), (**b**) Shymnagar (polder 15), (**c**) Amtali (polder 45), (**d**) Kukri-Mukri, (**e**) Mirersarai (polder 61/2), (**f**) Boro Moheshkhali (polder 69). Basemaps by Google Earth (2024).

At the west of the country, the sites with most potential to be integrated into dike designs are located at the southwest of polder 7/1 (Shahnagar) (Figure 5a), with a mean width of 206 m and a maximum width of 376 m, and on the south of polder 15 (Shymnagar) (Figure 5b), with a mean width of 234 m, and a maximum width of 351 m.

At the center of the country, seven patches with widths exceeding 1 km were identified, which largely shelter coastal embankments from cyclones. The largest two are located just south from polder 45 (Amtali) (Figure 5c), with a mean length of 1.77 km and a maximum length of 3 km, and a mangrove belt surrounding the Kukri-Mukri polder, with a mean width of 1.82 km and a maximum width of 2.9 km (Figure 5d).

At the east of the country, three sites had widths longer than 1 km. Sandwip has wide mudflat areas surrounding the north and north-east of polder 72 (with a mean length of 1.3 km), and their suitability for mangroves could be investigated in local assessments. The plantations of Mirersarai (Figure 5e) can significantly shelter the embankments that surround polder 61/2, with a mean forest width of 1.2 km. The mangroves surrounding polder 69 (Boro Moheshkhali) can also protect coastal embankments from the impact of extreme events, with mean forest widths of 1.4 km and maximum widths of 3.5 km (Figure 5f).

4. Discussion

4.1. Economic Benefits of Mangrove Belts

Concrete revetments are the most costly component of coastal embankments in Bangladesh. By leveraging the wave-damping benefits provided by existing mangroves, these revetments could be downsized or even eliminated, while maintaining the same level of safety. The cost of revetments has risen significantly in recent years, and future sea level rise will necessitate substantial investments to upgrade embankments and revetments. Rectangular concrete blocks of 40 × 40 × 20 cm with geotextiles have a cost of 20 USD m^{-2} (USD 2010) [33], corresponding with approximately 28 USD m^{-2} in 2024. For a dike with a height of 5 m and a slope of 1:3, revetment costs would be USD 238 per linear meter. Considering a section fronted by a mangrove belt with average width of 1.8 km, length of 22 km, and a total area of approximately 400 ha (representative of the widest belts in the center of the country), revetment costs along the mangrove section would be 522,716 USD (approximately 1400 USD ha^{-1}), neglecting the effect of mangroves. This 1.8 km mangrove belt could decrease the required revetment thickness by 80%. Such reduction does not directly translate to a linear decrease in cost (i.e., to a revetment cost reduction of 1120 USD ha^{-1}), as revetments are typically provided in fixed class sizes and weights. However, it could significantly lower expenses by allowing for the use of lighter revetment alternatives. With the largest wave load reductions around 80%, for some stretches only a few tens of cm wave height remains. This could well be stable without a concrete revetment, relying instead on just clay and grass covers [34].

By replacing a concrete revetment with mangroves, not only are the largest carbon emissions associated with revetment construction avoided [35], but mangroves also contribute additional carbon sequestration [9]. For context, the total carbon stock in mangrove plantations in Bangladesh in 2023 was estimated at 190 Mg C ha^{-1} across all monitored plantations [9]. This includes 60 Mg C ha^{-1} stored in biomass and 130 Mg C ha^{-1} as soil organic carbon. Carbon stocks varied across the coastal system, with averages of 174.5 Mg C ha^{-1} in the east, 152 Mg C ha^{-1} in the center, and 243.7 Mg C ha^{-1} in the west (particularly in plantations just east of the Sundarbans) [9]. Although these values are lower than those for natural mangroves in the Sundarbans (369 Mg C ha^{-1} [9]), they remain within the potential range for natural mangrove ecosystems.

Moreover, even if existing mangroves are not currently considered in embankment designs, they are likely reducing embankment maintenance costs at the locations where they are already present, such as those highlighted in Figure 5. In Vietnam, avoided embankment repair costs due to mangrove presence ranged from USD 80,000 to 295,000 for sites between 100–900 ha, corresponding with 327–800 USD ha^{-1} (the reference year was not specified) [36]. Similar assessments, comparing costs at sites with and without mangroves, and evaluating the cost reduction as a function of the forest properties, could also be performed in Bangladesh to quantify the value provided by existing mangrove forests.

In this study, we evaluated the maximum wave reduction potential of existing mangrove areas assuming that mangroves were healthy, but some sites may be degraded and require restoration interventions. Comparing potential mangrove belt benefits to restoration costs, historical data on mangrove restoration costs indicate that afforestation of 120,000 hectares between 1980 and 1990 cost USD 20 million, equivalent to 167 USD ha^{-1} in 1998 (approximately 320 USD ha^{-1} in 2024). At large sites requiring restoration efforts, the benefits of reduced revetment costs or decreased maintenance requirements could outweigh these restoration costs. However, in narrower forests, mangroves may be less cost-efficient. Additionally, restoration costs may be higher when further interventions beyond planting are required.

4.2. Limitations of Vegetation Models

The wave model assumed wave propagation across transects and did not account for potential 2D wave effects, such as diffraction or refraction caused by alongshore variations in bathymetry. As a result, the model's accuracy is expected to be higher in areas with uniform bathymetry and lower in regions with significant variability. Moreover, our focus was on the role of mangroves in wave attenuation, using constant surge levels, based on the fact that mangroves are more effective at reducing short waves than storm surges, and that complete surge attenuation is unfeasible given the relatively narrow mangrove fringes considered in this study and the large surge heights in Bangladesh. However, more detailed designs should account for wave–current interactions and evaluate surge propagation.

Additionally, we assumed uniform vegetation characteristics, whereas differences in vegetation properties, such as tree density, are known to influence wave attenuation [37]. For this study, we modeled mangroves with geometric properties of *Sonneratia apetala* trees measured at the east of the country (Table 2). However, the potential sites north from the Sundarbans neighbor regions are largely inhabited by *Heritiera fomes* and *Excoecaria agallocha*, with different geometries and associated wave damping properties. Spatial variations in forest properties can be inferred from biomass differences across the country [9]. Biomass comparisons show similarities between the center and east of Bangladesh, except near the Sundarbans, where biomass nearly doubles. This suggests potentially higher wave reduction rates than predicted at sites with larger biomass [9]. The effect of varying vegetation properties is likely most important for small belt widths, and less so for wider belts that attenuate most wave energy [8,38].

Existing mangroves can also degrade over time in response to natural and anthropogenic effects. Plantations near the Sundarbans have shown the steepest growth curves and highest survival rates, of 42.5%, while survival rates decrease down to 10.5% eastwards. Overall, the central region is where most plantations are expected in the future, extrapolating from current plantation rates. Accretion and coastal expansion are also largest near the mouth of the Meghna River, offering opportunities for mangrove establishment. Nevertheless, coastal evolution under climate change is uncertain. According to the literature, Bangladesh has been accreting more than eroding during the last decades [39], but future sediment supply and its distribution across the coastal system are likely to change with sea level rise and changes in river runoff.

4.3. Recommendations for Future Studies

Additional opportunities could be identified by considering mangrove restoration techniques that expand the mangrove habitat, such as the conversion of shrimp ponds into mangrove forests or realigning embankments to expand mangrove plantations landwards. At sites where existing mangrove vegetation can be integrated into hybrid embankment designs, local studies should assess mangrove conditions and plan restoration interventions if needed.

For future studies, we recommend assessing the effect of mangroves on embankments using 2D flow and wave models, which will provide more accurate assessments at sites with complex flows (e.g., at sites near estuaries, with non-uniform coastal morphologies and forest shapes). Local ecological studies and local mangrove measurements will help to improve more accurate assessments of vegetation performance. Given that mangrove plantations are already present across the country, obtaining more insight in how they influence coastal morphology, stability and sediment retention is recommended as this may be crucial to mitigate coastal erosion under sea level rise. Information on mangrove resilience, by surveying damage to trees before and after typhoons and storms, provides valuable insights in how resilient these ecosystems are under extreme weather conditions.

5. Conclusions

This study quantifies the benefits of integrating mangrove belts into coastal flood defenses in Bangladesh. Our analysis shows that mangroves can substantially reduce the thickness of embankment revetments—up to 82% in key areas like Kukri-Mukri and Amtali—and decrease shear stresses by up to 97%. The advantages of mangrove presence are most pronounced in the central and eastern regions, where wider mangrove belts are more effective at mitigating wave energy and lowering embankment design requirements. In contrast, the western region, with narrower mangrove belts, shows more modest benefits. Integrating mangroves into coastal protection systems can lead to significant cost savings besides providing other benefits like avoided carbon emissions (due to the replacement of concrete revetments) and carbon sequestration, among other ecosystem services. Future efforts should focus on investigating mangrove areas in high-benefit regions and refining numerical models and predictive capacity on the role and resilience of mangroves with local data. This approach not only strengthens coastal defenses but also promotes environmental sustainability for safeguarding Bangladesh's vulnerable coastal communities.

Author Contributions: A.G.M. developed the model, analyzed model results, and wrote the manuscript. B.A.J., B.K.v.W., and B.H. wrote and edited the manuscript and S.K. and I.U. provided the project's funding. All authors have read and agreed to the published version of the manuscript.

Funding: The research was funded by a grant received by the World Bank through the European Union and managed by the Global Facility for Disaster Reduction and Recovery (GFDRR).

Institutional Review Board Statement: Not applicable.

Informed Consent Statement: Not applicable.

Data Availability Statement: Data can be made available upon consultation.

Acknowledgments: The authors would like to thank the TU Delft and World Bank peer reviewers for their comments.

Conflicts of Interest: The authors declare no conflicts of interest.

References

1. Eckstein, D.; Künzel, V.; Schäfer, L.; Winges, M. *Global Climate Risk Index 2019*; Germanwatch e.V.: Bonn, Germany, 2020.
2. ICPP. *Climate Change 2007: Impacts, Adaptation and Vulnerability: Summary for Policymakers. Working Group II Contribution to the Intergovernmental Panel on Climate Change Fourth Assessment Report*; ICPP: Geneva, Switzerland, 2007.
3. Menéndez, P.; Losada, I.; Torres-Ortega, S.; Narayan, S.; Beck, M. The Global Flood Protection Benefits of Mangroves. *Sci. Rep.* **2020**, *1*, 1–11. [CrossRef] [PubMed]
4. van Zelst, V.T.; Dijkstra, J.T.; van Wesenbeeck, B.K.; Eilander, D.; Morris, E.P.; Winsemius, H.C.; de Vries, M.B. Cutting the costs of coastal protection by integrating vegetation in flood defences. *Nat. Commun.* **2021**, *12*, 6533. [CrossRef] [PubMed]
5. Tiggeloven, T.; de Moel, H.; van Zelst, V.; van Wesenbeeck, B.; Winsemius, H.; Eilander, D.; Ward, P. The benefits of coastal adaptation through conservation of foreshore vegetation. *J. Flood Risk Manag.* **2022**, *15*, e12790. [CrossRef]
6. Saenger, P.; Siddiqi, N. Land from the sea: The mangrove afforestation program of Bangladesh. *Ocean. Coast. Manag.* **1993**, *20*, 23–39. [CrossRef]
7. Crawford, T.; Islam, M.; Rahman, M.; Paul, B.; Curtis, S.; Miah, M.; Islam, M. Coastal Erosion and Human Perceptions of Revetment Protection in the Lower Meghna Estuary of Bangladesh. *Remote Sens.* **2020**, *12*, 3108. [CrossRef]
8. Gijón Mancheño, A.; Vuik, V.; van Wesenbeeck, B.K.; Jonkman, S.N.; van Hespen, R.; Moll, J.R.; Kazi, S.; Urrutia, I.; van Ledden, M. Integrating mangrove growth and failure in coastal flood protection designs. *Sci. Rep.* **2024**, *14*, 7951. [CrossRef]
9. Uddin, M.; Aziz, A.; Lovelock, C. Importance of mangrove plantations for climate change mitigation in Bangladesh. *Glob. Change Biol.* **2023**, *29*, 3331–3346. [CrossRef]
10. Brander, L.; Wagtendonk, A.; Hussain, S.; McVittie, A.; Verburg, P.; de Groot, R.; van der Ploeg, S. Ecosystem service values for mangroves in Southeast Asia: A meta-analysis and value transfer application. *Ecosyst. Serv.* **2012**, *1*, 62–69. [CrossRef]

11. Dasgupta, S.; Huq, M.; Huq Khan, Z.; Zahid Ahmed, M.; Mukherjee, N.; Khan, M.; Pandey, K. *Vulnerability of Bangladesh to Cyclones in a Changing Climate: Potential Damages and Adaptation Costs*; Technical report; Policy Research Working paper 5280; The World Bank Development Research Group, Environment and Energy Team: Washington, DC, USA, 2010.
12. Méndez, F.; Losada, I. An empirical model to estimate the propagation of random breaking and nonbreaking waves over vegetation fields. *Coast. Eng.* **2004**, *51*, 103–118. [CrossRef]
13. Iftekhar, M.; Saenger, P. Vegetation dynamics in the Bangladesh Sundarbans mangroves: A review of forest inventories. *Wetl. Ecol. Manag.* **2008**, *16*, 291–312. [CrossRef]
14. Biswas, S.; Choudhury, J.; Nishat, A.; Rahman, M. Do invasive plants threaten the Sundarbans mangrove forest of Bangladesh? *For. Ecol. Manag.* **2007**, *245*, 1–9. [CrossRef]
15. Uddin, M.; Hossain, M.; Aziz, A.; Lovelock, C. Ecological development of mangrove plantations in the Bangladesh Delta. *For. Ecol. Manag.* **2022**, *517*, 120269. [CrossRef]
16. Dutta, D.; Das, P.K.; Paul, S.; Sharma, J.R.; Dadhwal, V.K. Assessment of ecological disturbance in the mangrove forest of Sundarbans caused by cyclones using MODIS time-series data (2001–2011). *Nat. Hazards* **2015**, *79*, 775–790. [CrossRef]
17. Rahman, M.; Rahman, M.; Islam, K. The causes of deterioration of Sundarban mangrove forest ecosystem of Bangladesh: Conservation and sustainable management issues. *AACL Bioflux* **2010**, *3*, 77–90.
18. Bolts, W. *Carte du Bengale et de ses dé Pendances*; Universität Bern: Bern, Switzerland, 1775.
19. Curtis, S. *Working plan for the forests of the Sundarbans Division for the period from 1st April 1931 to 31st March 1951, Volume III Part of Appendix III Description of the Compartments and their Histories*; Government of Bengal: Kolkata, India, 1933.
20. Hoque, A.; Datta, D. The mangroves of Bangladesh. *Wetl. Sci. Pract.* **2005**, *31*, 45–253.
21. Hossain, M.; Lin, C.; Hussain, M. Goodbye Chakaria Sunderban: The Oldest Mangrove Forest. *Wetl. Sci. Pract.* **2009**, *18*, 19–22. [CrossRef]
22. UBINIG. Available online: https://ubinig.org/index.php/home/showAerticle/211/english/UBINIG/Protection-of-Mangrove-forest (accessed on 30 October 2023)
23. Uddin, M.M.; Rahman, M.S.; Hossain, K.; Akter, S. Growth density and regeneration of afforested mangroves at Mirersarai forest range in Bangladesh. *For. Sci. Technol.* **2014**, *10*, 120–124. [CrossRef]
24. IWM. *Technical Report on Storm Surge, Wave, Hydrodynamic Modelling and Design Parameters on Drainage System and Embankment Crest Level. Volume-II: Package 2 (Appendix-B: Storm Surge)*; Technical Report; Bangladesh Water Development Board, Ministry of Water Resources: Dhaka, Bangladesh, 2018.
25. Thornton, E.; Guza, R. Transformation of Wave Height Distribution. *J. Geophys. Res.* **1983**, *88*, 5925–5938. [CrossRef]
26. Van Wesenbeeck, B.; Wolters, G.; Antolinez, J.; Kalloe, S.; Hofland, B.; de Boer, W.; Çete, C.; Bouma, T. Wave attenuation through forests under extreme conditions. *Sci. Rep.* **2022**, *12*, 1884. [CrossRef]
27. Van der Meer, J.; Allsop, N.; Bruce, T.; De Rouck, J.; Kortenhaus, A.; Pullen, T.; Schuttrumpf, H.; Troch, P.; Zanuttigh, B. Manual on Wave Overtopping of Sea Defences and Related Structures. Technical Report, An Overtopping Manual Largely Based on European Resreach, but for Worldwide Application. EurOtop, 2018. Available online: www.overtopping-manual.com (accessed on 20 October 2023).
28. Pilarczyk, K. *Coastal Protection*; A.A. Balkema: Rotterdam, The Netherlands, 1990.
29. Pilarczyk, K. *Dikes and Revetments*; A.A. Balkema: Rotterdam, The Netherlands, 1998.
30. D-Morphology User Manual. Version 2023 of 8th December 2022. Available online: https://content.oss.deltares.nl/dhydro/D-Morphology_User_Manual.pdf (accessed on 20 October 2023).
31. Krauss, K.; Osland, M. Tropical cyclones and the organization of mangrove forests: A review. *Ann. Bot.* **2020**, *125*, 213–234. [CrossRef]
32. Montgomery, J.M.; Bryan, K.R.; Mullarney, J.C.; Horstman, E.M. Attenuation of storm surges by coastal mangroves. *Geophys. Res. Lett.* **2019**, *46*, 2680–2689. [CrossRef]
33. Alam, M.; Hasan, M. Protection Works Against Wave Attacks in the Haor Areas of Bangladesh: Analysis of Sustainability. *J. Constr. Dev. Ctries.* **2010**, *15*, 69–85.
34. Schiereck, G.; Verhagen, H. *Introduction to Bed, Bank and Shore Protection*; Coastal Engineering (CEG) (TU Delft): Delft, The Netherlands, 2019.
35. Arbeláez Pérez, O.; Senior Arrieta, V.; Gómez Ospina, J.; Herrera Herrera, S.; Ferney Rodríguez Rojas, C.; Santis Navarro, A. Carbon dioxide emissions from traditional and modified concrete. A review. *Environ. Dev.* **2024**, *52*, 101036. [CrossRef]
36. IFRC. Case Study Mangrove Plantation in Viet Nam: Measuring Impact and Cost Benefit; Technical Report. Available online: https://ifrc-media.org/interactive/mangrove-plantation-in-viet-nam-measuring-impact-and-cost-benefit/ (accessed on 20 October 2023).
37. Bao, T. Effect of mangrove forest structures on wave attenuation in coastal Vietnam. *Oceanologia* **2011**, *53*, 807–818.

38. Vuik, V.; Borsje, B.W.; Willemsen, P.W.; Jonkman, S.N. Salt marshes for flood risk reduction: Quantifying long-term effectiveness and life-cycle costs. *Ocean. Coast. Manag.* **2019**, *171*, 96–110. [CrossRef]
39. Sarwar, M.; Woodroffe, C. Rates of shoreline change along the coast of Bangladesh. *J. Coast. Conserv.* **2013**, *17*, 515–526. [CrossRef]